R. & M. No. 2883
(13,632)
A.R.C. Technical Report

MINISTRY OF SUPPLY

AERONAUTICAL RESEARCH COUNCIL
REPORTS AND MEMORANDA

An Experimental Investigation of a Thick-Aerofoil Nozzle Cascade

By

S. J. ANDREWS, B.Sc.
and
N. W. SCHOFIELD

LONDON: HER MAJESTY'S STATIONERY OFFICE
1956
FOUR SHILLINGS NET

An Experimental Investigation of a Thick-Aerofoil Nozzle Cascade

By

S. J. ANDREWS, B.Sc.

and

N. W. SCHOFIELD

COMMUNICATED BY THE PRINCIPAL DIRECTOR OF SCIENTIFIC RESEARCH (AIR), MINISTRY OF SUPPLY

Reports and Memoranda No. 2883*

May, 1950

Summary.—The cascade tests on a thick-aerofoil turbine nozzle blade suitable for a cooled turbine show that it has a good performance over a wide incidence range up to $M = 0{\cdot}8$. Above this value the loss coefficient rises and does not fall again as $M = 1$ is approached. Several methods of indication of the transition point have been tried and results show that the method depending on the evaporation of crystals gives a position inconsistent with three other methods, *i.e.*, lamp-black deposit, surface total-head measurement and stethoscope search tube.

The effect of the thick trailing edge on loss coefficient is almost that predicted assuming zero velocity behind the blade trailing edge. The heat-transfer increase due to transition is probably not large, and is no worse than that on a conventional turbine section.

1. *Introduction.*—In order to design a successful high-temperature turbine blade a considerable thickness toward the trailing edge is required so that this part of the blade may be effectively cooled. An aerofoil-section blade with the thickness maintained well toward the trailing edge (Fig. 1) has, therefore, been tested in cascade as a nozzle row. The flow over the blade surfaces has been investigated to determine the transition point, and theoretical estimates of the effect of the thick trailing edge have been made, so that the heat-transfer properties and efficiency of such blades can be estimated.

2. *Cascade Performance.*—The cascade which has been tested on No. 4 High-Speed Cascade Tunnel has its geometrical properties and range of tests given below

β_1	=	+2 deg
β_2	=	−59 deg
ζ	=	38·6
s/c	=	0·65
t/c	=	0·185
l	=	3·0 in.
c	=	1·5 in.
Camber	=	P40

Range of Tests

Inlet angle	−35 deg to +35 deg
Mach number	0·3 to 0·9
Reynolds number	2·6 to 7·8 × 10^5

(No turbulence factor)

with the aerofoil shape shown in Fig. 1.

* N.G.T.E. Memorandum M.84, received 30th December, 1950.

The general performance curves of the cascade are shown in Figs. 2 and 3 which have gas inlet angle, and inlet Mach number respectively as abscissa. These curves show that the blade stalls at an inlet angle of +30 deg for Mach numbers above 0·4 and below 0·8 but this stall has very little effect on the gas outlet angle. The same can be said taking M as a variable; the loss begins to increase fairly quickly above $M = 0{\cdot}8$ with again little apparent effect on the outlet angle.

2.1. *Comparison with Other Results.*—The cascade being considered is not unlike the cascade No. 4. Ref. 1, the main difference being the flat on the trailing convex surface of the latter which is made up of circular arcs and a straight line, *i.e.*, a conventional turbine section. The performance of the aerofoil cascade is better than that of the conventional cascade up to $M = 0{\cdot}9$. At this speed, the loss coefficient of the aerofoil blade is rising fairly steeply but that of the conventional blade is tending to decrease. This comparative performance between flat and curved back types of section seems to be characteristic.

Cascade details						Mach number 0·6		Mach number 0·9		Mach number 1·0
	c (in.)	T.E./c	t/c	β_2 (deg)	α_1 (deg)	$\bar{\omega}/\frac{1}{2}\rho V_2^2$	α_2	$\bar{\omega}/\frac{1}{2}\rho V_2^2$	α_2	$\bar{\omega}/\frac{1}{2}\rho V_2^2$
No. 4, Ref. 1	1·8	0·008	0·180	—58	+10	0·032	56	0·040	57	0·035
Aerofoil	1·5	0·037	0·185	—59	+10	0·024	62	0·040	62	>0·10

In terms of maximum lift drag ratio the aerofoil cascade is 40 per cent better than the conventional cascade. The aerofoil has a maximum lift drag ratio of 72 occurring at $M = 0{\cdot}7$ whereas the corresponding values for the conventional cascade are 52 at $M = 0{\cdot}6$.

In Ref. 2, p. 234, a curve is shown giving the effect of Mach number on outlet angle. The agreement between this curve and the results obtained is good for low speeds only, because the tendency for the outlet angle to approach $\cos^{-1} o/s$ as the Mach number tends to unity, does not occur.

2.2. *Effect of Trailing-Edge Thickness.*—The cascade two-dimensional loss consists of two main parts, that due to blade-surface friction and that due to the wake from the thick trailing edge. In order to determine the relative size of these quantities, a theoretical investigation of the friction loss and wake loss have been made.

H.B. Squire, Ref. 3, gives a method by which the laminar boundary-layer details can be found once the velocity distribution over the blade surface is known. This velocity distribution was found by means of blade-surface static-pressure measurement and is shown in Fig. 7 together with the boundary-layer momentum thickness. From the momentum thickness at outlet, the loss corresponding to a blade with a perfectly sharp trailing edge is obtained. Then from Ref. 4 is found the additional loss due to a trailing edge of finite thickness, assuming zero velocity immediately behind the trailing edge and uniform static pressure across wake and blade passage. This method of loss estimation by treating friction and trailing-edge loss separately gives a total loss coefficient of only 86 per cent of that actually measured and the ratio of trailing-edge loss to total loss is as 0·4 is to 1·0.

$\alpha_1 = -4{\cdot}5$ deg ; $R_e = 5 \times 10^5$; T.E. thickness/s	=	0·056
Theoretical friction loss coefficient	=	1·2 per cent
Additional loss due to T.E. thickness	=	0·8 per cent
Total		2·0 per cent
Measured loss coefficient	=	2·3 per cent

3. *Indication of Transition.*—The indication of transition point or region has been carried out by several different methods which are described briefly below.

Evaporation.—In a turbulent boundary layer there is, by definition, a continuous interchange of the air next to the surface with that lying nearest the free stream, as opposed to the laminar boundary layer where the flow is of a shearing nature. The turbulence can, therefore, cause a very much greater degree of evaporation from the surface than the laminar flow and this fact is used to indicate regions of turbulence.

The method (Ref. 5) is to spray on to the blade surface a solution of p-diethoxybenzene in petroleum which, when evaporated, deposits on the surface a layer of small white crystals. These crystals are themselves volatile and if the airflow is turbulent over any part of the blade surface, then the greater rate of evaporation in this region will cause the crystals to disperse, leaving the laminar area still covered with a white deposit. The complete change will occur in from 10 to 40 minutes depending on the crystal-layer thickness (Fig. 9).

Lamp-Black Deposition.—It has been found that an extremely thin deposit of lamp-black will be lifted from the surface in a turbulent boundary layer and will remain unaffected in the presence of a laminar layer. The lamp-black was, in this instance, deposited from an acetylene flame and this was completely removed in approximately 10 to 20 seconds by a turbulent boundary leaving the laminar region black, giving therefore a sharp and photographable transition line (Fig. 8).

Boundary-Layer Total-Head Measurement.—A total-head tube of dimensions smaller than the boundary thickness will read a pressure which is dependant on the boundary-layer shape when placed on the blade surface facing upstream. In a laminar boundary layer where the rate of change of velocity normal to the blade surface (du/dn) is comparatively small the pressure readings will be small, whereas in a turbulent layer (du/dn) is large, and gives a correspondingly large total-head pressure reading. Taking for example the traverse from a laminar region to a turbulent region. The pitot pressure will first be small and decreasing showing a tendency for the boundary layer to separate. If, however, transition occurs first, the total head will rise steeply from the minimum point (*see* Fig. 4c). Contours of readings given by such a traverse, repeated at different positions along the blade length, give the transition region.

Stethoscope and Microphone Search Instruments.—A stethoscope attached to a small pitot tube as mentioned above, and traversed in a similar manner, will indicate a considerable change in the noise level and character as the pitot-tube moves from the laminar to the turbulent layer.

Another device of essentially similar nature is the microphone pick-up, the output of which when applied to a cathode-ray oscilloscope shows clearly the production of pressure pulses in a turbulent layer.

3.1. *Comparison of Methods of Indication.*—All forms of the above methods have been applied to the turbine cascade working at moderate speed and inlet angle of —4·5 deg. There is a good agreement between the lamp-black, total-head tube and stethoscope methods for indicating the position of transition, but the evaporation method gives a somewhat different result.

The transition as shown by evaporation is at $x/c = 0 \cdot 07$ (low speed) forward from the trailing edge, whereas the other three methods indicate a transition point at $x/c = 0 \cdot 12$ from the trailing edge. A possible explanation of the effect is that the growth of turbulence is slow and only arrives at a state where elements of the boundary layer undergo complete and continuous interchange, after a definite distance, depending on the pressure gradient.

The microphone search-tube suggests another explanation. When this instrument is placed on the transition line indicated by the lamp-black it registers only bursts of unsteadiness. It is possible therefore that the lamp-black indicates the forward limit of intermittent turbulence while the evaporation method indicates a continuous turbulent state. The microphone tests were carried out while this report was in preparation so conclusions on the incomplete tests cannot be definite.

Fig. 4a shows the agreement between the total-head tube and lamp-black methods for transition indication at low speeds. Fig. 6 shows a total-head traverse in two types of turbulence wedge. The first type, which can be produced by a large rounded particle on the blade surface, has a centre portion with, apparently, a new laminar boundary layer originating from the particle. The second type originates from undetectable irregularities on the surface. The relative angle of wedge as shown is a true reproduction of those observed.

4. *The Transition Point.*—4.1. *The Effect of Incidence.*—As will be seen from the photographs in Fig. 8 and 9, there is little incidence effect on the convex-surface transition point from an inlet angle of -34 deg to $+19$ deg the variation being between $x/c = 0 \cdot 12$ and $0 \cdot 18$ from the trailing edge. The concave surfaces corresponding to those mentioned above are completely black except for an inlet angle of -34 deg. In this instance the concave surface is devoid of soot from $x/c = 0 \cdot 1$ from the stagnation point to an indefinite line at $x/c = 0 \cdot 4$. This indicates early transition followed by turbulent separation. At a high positive inlet angle ($\alpha_1 = 34$ deg) a similar sequence of events occur, but this time on the convex surface. Transition takes place at $x/c = 0 \cdot 03$ from the stagnation point and separation at $x/c = 0 \cdot 70$.

4.2. *The Effect of a Turbulent Inlet.*—To determine this effect the cascade was mounted at outlet from an unlit combustion chamber. The velocity distribution at this section is shown in Fig. 5 together with the blade surface total-head distribution. The transition point moved toward the leading edge to a position $x/c = 0 \cdot 33$ from the trailing edge (cascade tunnel value $x/c = 0 \cdot 12$). Again the evaporation method of indicating transition gave results inconsistent with other methods. It is interesting to note in Fig. 5 that the blade-surface total-head distribution for a turbulent inlet is similar to that obtained on the end blade of the cascade, over the back of which the tunnel-wall boundary layer flows, shown in Fig. 6.

Summary of Transition Point Results

$\alpha_1 = -4 \cdot 5$ deg Mach number between $0 \cdot 5$ and $0 \cdot 7$
Transition-point distance from trailing edge as a proportion of the chord.

Cascade Tunnel Inlet	x/c
Total-head traverse over surface	$0 \cdot 115$
Lamp-black	$0 \cdot 120$
Stethoscope	approx. $0 \cdot 11$
Evaporation	$0 \cdot 065$

Combustion Chamber Inlet	x/c
Total-head traverse over surface	$0 \cdot 30$
Lamp-black	$0 \cdot 33$
Stethoscope	approx. $0 \cdot 30$
Evaporation	$0 \cdot 15$

4.3. *Theoretical Prediction of Separation and Instability.*—As mentioned in section 2.2 the velocity distribution round the blade is found from static-pressure tappings on the blade surface. The static holes themselves are 0·02 in. in diameter and eleven of these are distributed on both concave and convex surfaces. From the velocity distribution, the momentum thickness of the boundary layer is found (Ref. 3), and by using a criterion due to Thwaites $((\theta^2/\nu)(du/dx) = -0{\cdot}07)$ Ref. 7, the point of separation of a laminar boundary layer can be estimated. This point is marked on the convex-surface velocity distribution, Fig. 7, and it occurs just upstream of the experimental transition point. The theory does not therefore agree well with the experimental result although from Fig. 4, it is evident that the surface total-head pressure does closely approach the local static pressure indicating a tendency to separate.

To estimate the transition point by theoretical methods is not easy, but using the Polhausen criterion the point of instability can be found from the velocity and boundary-layer momentum-thickness distributions (Ref. 6). This point is also marked in Fig. 7 and occurs just downstream of the minimum pressure point. Apart from this it has no particular experimental significance.

5. *The Effect of Turbulence on Heat Transfer.*—From the results obtained above it is evident that turbulent flow conditions would exist over $x/c = 0{\cdot}30$ of the blade top surface, if used in an engine. This would be bad from the point of view of blade cooling as, for several reasons, the trailing edge is the most difficult part of the blade in which to put a cooling passage. However, it is fairly certain that if evaporation from the surface is not at a high rate, then heat transfer is similarly not at a high rate, it can then be inferred from the above table that high heat transfer corresponding to fully developed turbulence will only exist over $x/c = 0{\cdot}15$ of the trailing edge.

6. *Conclusions.*—(*a*) This aerofoil nozzle blade gives a good performance below an outlet Mach number of 0·8 over a wide range of incidence. Above $M = 0{\cdot}8$, however, the loss increased fairly steeply and does not decrease with the approach of sonic speed, as with the conventional flat-back type of blade.

(*b*) Below $M = 0{\cdot}8$ the nozzle would be very suitable for an internally cooled blade of a high-temperature turbine, being comparatively thick quite far back toward the trailing edge.

(*c*) Transition to turbulence on this blade with the cascade mounted at exit from an unlit combustion chamber begins at $x/c = 0{\cdot}33$ from the trailing edge and becomes fully developed, *i.e.*, high probable heat-transfer coefficient, at $x/c = 0{\cdot}15$ from the trailing edge. This undesirable state of affairs exists with most turbine blades and is no worse than usual in this case.

(*d*) The loss due to the thick trailing edge $(t/s \cos \alpha_2 = 0{\cdot}119)$ is approximately that predicted assuming zero velocity immediately behind the trailing edge. In this instance the trailing edge contributes 0·008 to the theoretical total loss coefficient of 0·020, *i.e.*, 40 per cent. Although the loss due to the trailing edge is a high proportion of the total loss, the value of the minimum total loss itself is less than that of a conventional blade of similar design.

(*e*) The indication of turbulence by the removal of lamp-black from blade has a greater physical significance than a method depending on evaporation under the above conditions, in that it defines a critical point in the boundary-layer growth. The result given by an evaporation method, however, is of practical use in indicating well-developed turbulence.

REFERENCES

No.	Author	Title, etc.
1	E. A. Bridle	Some high-speed tests on turbine cascades. R. & M. 2697. February, 1949.
2	D. G. Ainley	Performance of axial-flow turbines. *Proc. I. Mech. E.*, Vol. 159, 1948.
3	H. B. Squire	Heat-transfer calculations for aerofoils. R. & M. 1986. November, 1942.
4	J. Reeman and E. A. Simonis	The effect of trailing-edge thickness on blade loss. R.A.E. Tech. Note Eng. 116.
5	R. C. A. Dando	Two methods of boundary-layer transition indication suitable for routine tests in flight. A.R.C. 12,531. April, 1949.
6	A. Walz	Approximation methods for the calculation of laminar and turbulent boundary layers. UM. 3060 (1943).
7	B. Thwaites	Approximate calculation of the laminar boundary layer. *The Aeronautical Quarterly*, Vol. 1, Part III. November, 1949.

NOTATION

s	Blade pitch
c	Blade chord
ζ	Stagger angle
β_1	Blade inlet angle
β_2	Blade outlet angle
α_1	Gas inlet angle
α_2	Gas outlet angle
t	Blade maximum thickness
o	Cascade throat width
x	Distance along blade surface
n	Distance normal to the blade surface
θ	Boundary-layer momentum thickness
ν	Kinematic viscosity
l	Blade length
u	Gas velocity inside the boundary layer
U	Free-stream gas velocity
M	Mach number
R_e	Reynolds number

Suffixes

1	Cascade inlet section
2	Cascade outlet section
s	On blade surface

APPENDIX I

Table of Results

α_1	−34·3	−34·3	−34·3	−34·3	−34·3	−34·3
M	0·30	0·51	0·60	0·71	0·80	0·92
α_2	61·7	61·9	62·0	62·0	62·2	62·4
$\bar{\omega}/P_{\text{tot}\,1} - P_a$	0·046	0·032	0·032	0·031	0·032	0·072
$\Delta P/P_{\text{tot}\,1} - P_a$	0·66	0·69	0·74	0·70	0·77	0·79
α_1	−19·2	−19·2	−19·2	−19·2	−19·2	−19·2
M	0·31	0·51	0·61	0·70	0·80	0·92
α_2	62·0	61·9	61·9	62·0	62·2	62·1
$\bar{\omega}/P_{\text{tot}\,1} - P_a$	0·031	0·028	0·027	0·027	0·027	0·068
$\Delta P/P_{\text{tot}\,1} - P_a$	0·73	0·76	0·79	0·80	0·83	0·85
α_1	−4·6	−4·6	−4·6	−4·6	−4·6	−4·6
M	0·28	0·52	0·59	0·70	0·81	0·91
α_2	61·5	61·5	61·6	61·7	62·2	62·0
$\bar{\omega}/P_{\text{tot}\,1} - P_a$	0·030	0·024	0·024	0·023	0·023	0·053
$\Delta P/P_{\text{tot}\,1} - P_a$	0·75	0·78	0·79	0·81	0·81	0·87
α_1	+4·6	+4·6	+4·6	+4·6	+4·6	+4·6
M	0·28	0·52	0·62	0·70	0·81	0·90
α_2	62·6	62·8	62·7	62·4	62·1	61·9
$\bar{\omega}/P_{\text{tot}\,1} - P_a$	0·032	0·024	0·023	0·024	0·026	0·041
$\Delta P/P_{\text{tot}\,1} - P_a$	0·74	0·77	0·79	0·81	0·84	0·86
α_1	+19·2	+19·2	+19·2	+19·2	+19·2	+19·2
M	0·30	0·52	0·61	0·70	0·81	0·91
α_2	62·3	62·4	62·3	62·2	62·1	61·9
$\bar{\omega}/P_{\text{tot}\,1} - P_a$	0·033	0·026	0·025	0·022	0·027	0·042
$\Delta P/P_{\text{tot}\,1} - P_a$	0·74	0·78	0·79	0·81	0·84	0·85
α_1	+34·3	+34·3	+34·3	+34·3	+34·3	+34·3
M	0·34	0·50	0·61	0·70	0·80	0·90
α_2	61·0	61·5	61·7	61·9	61·9	62·2
$\bar{\omega}/P_{\text{tot}\,1} - P_a$	0·042	0·040	0·042	0·043	0·044	0·068
$\Delta P/P_{\text{tot}\,1} - P_a$	0·59	0·70	0·72	0·74	0·80	0·80

P_{tot}	Total pressure
P_{stat}	Static pressure
P_a	Atmospheric pressure
ΔP	$P_{\text{stat}\,1} - P_a$

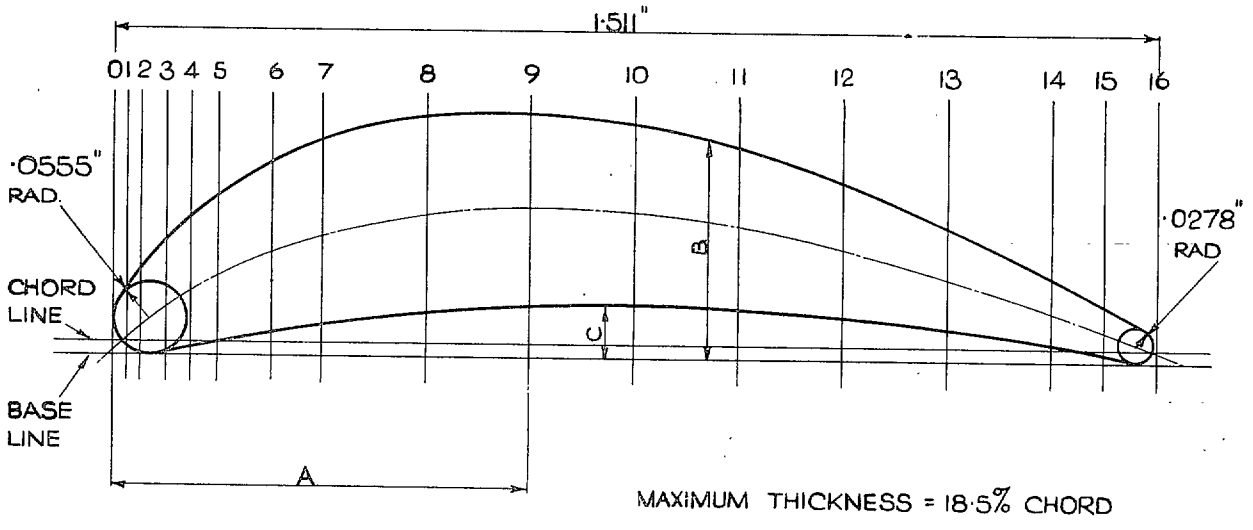

STATION	0	1	2	3	4	5	6	7	8	9	10	11	12	13	14	15	16
A	0	·0189	·0378	·0755	·1133	·1511	·2266	·3022	·4533	·6044	·7555	·9066	1·0577	1·2088	1·3599	1·4354	1·5110
B	·0565	·1052	·1335	·1780	·2107	·2375	·2787	·3075	·3450	·3530	·3422	·3125	·2640	·2015	·1285	·0870	·0290
C	·0565	·0140	·0032	·0025	·0085	·0155	·0332	·0485	·0677	·0755	·0735	·0670	·0572	·0412	·0210	·0087	·0290

FIG. 1. Turbine blade section.

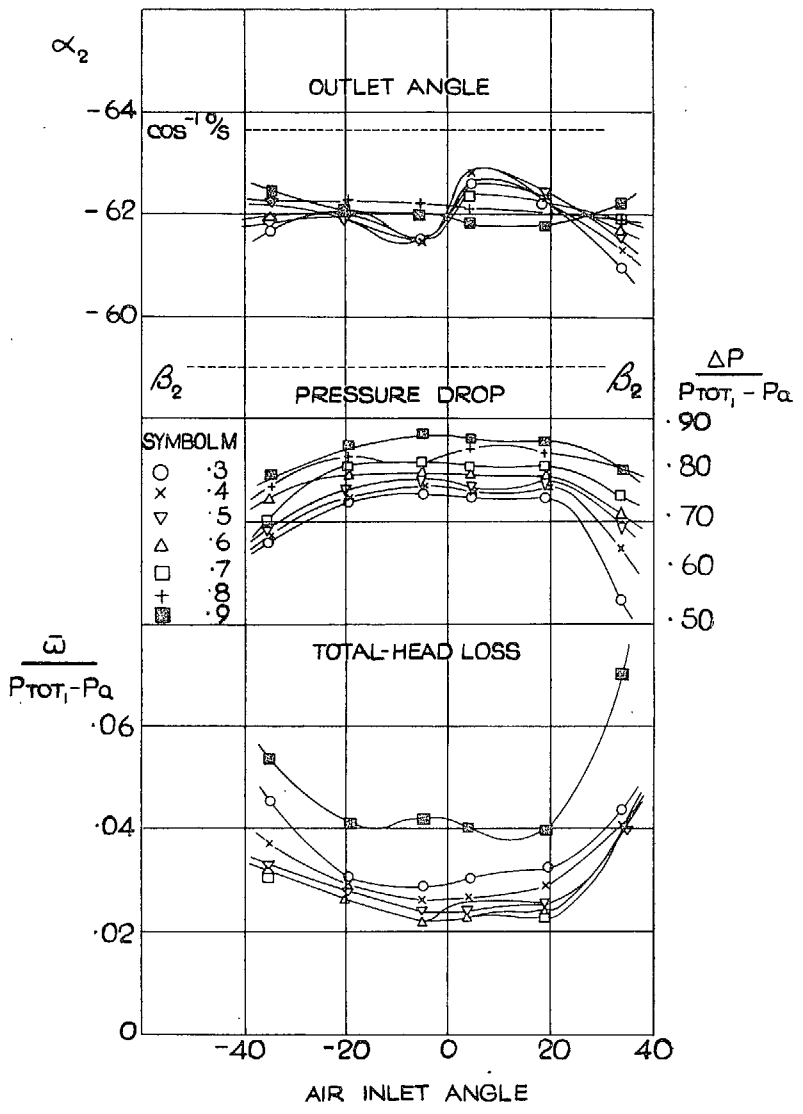

FIG. 2. Turbine nozzle cascade performance (α_1 abscissa).

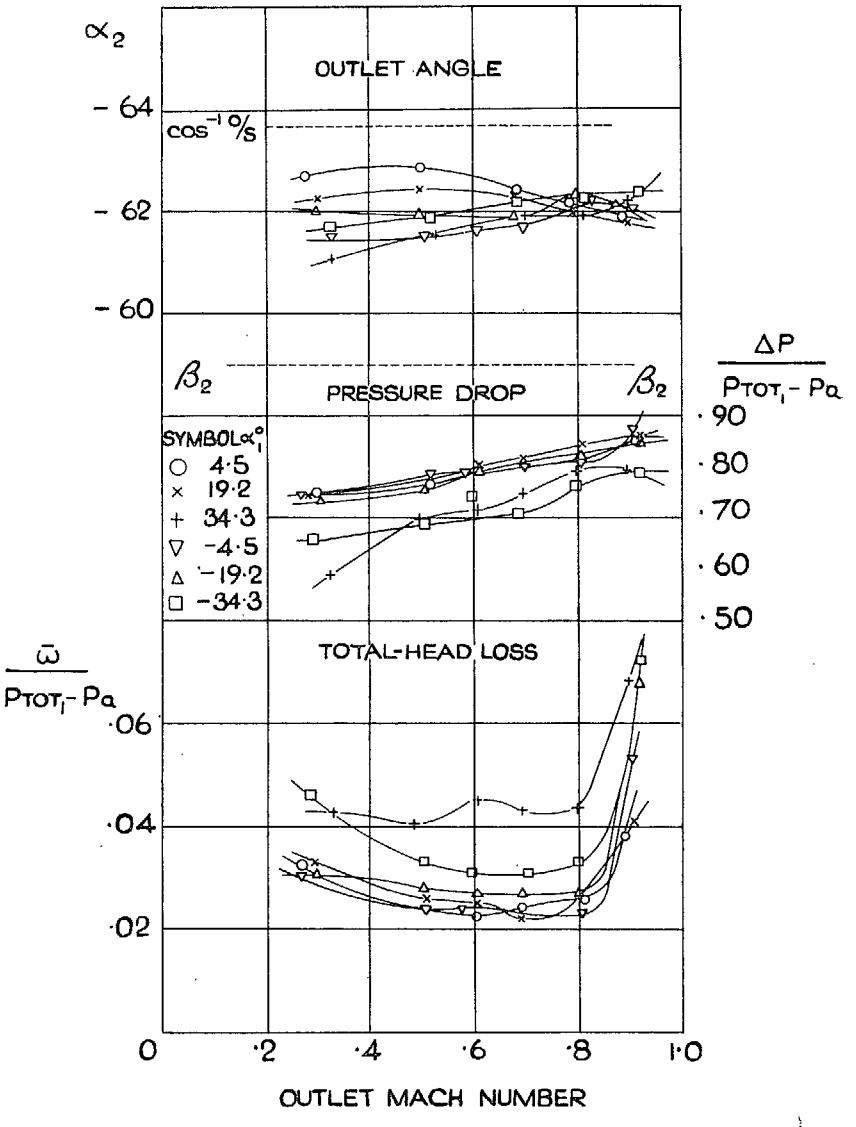

FIG. 3. Turbine nozzle cascade performance (M abscissa).

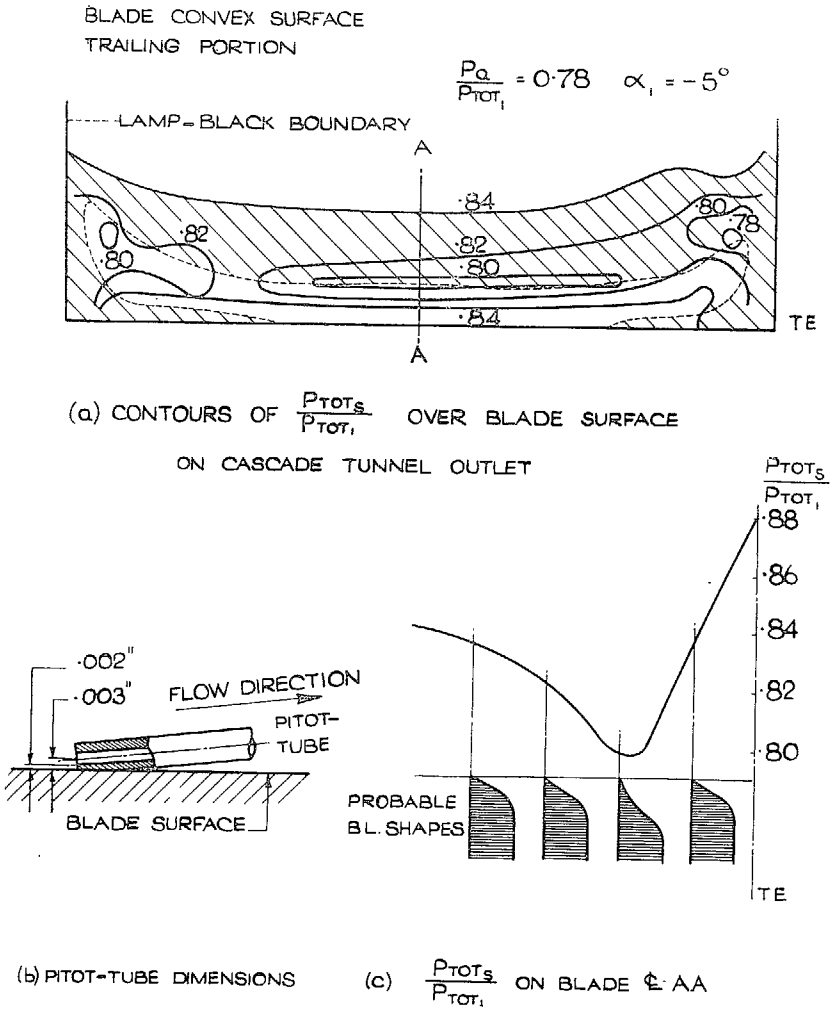

FIG. 4. I Blade surface total-pressure measurements.

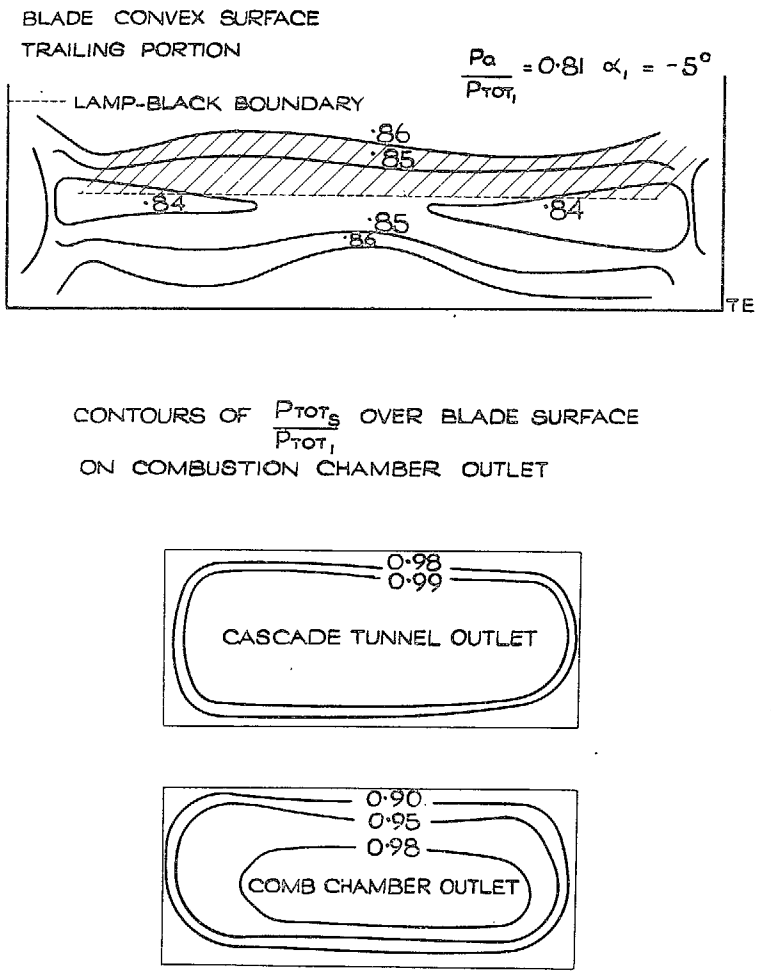

FIG. 5. II Blade surface total-pressure measurements.

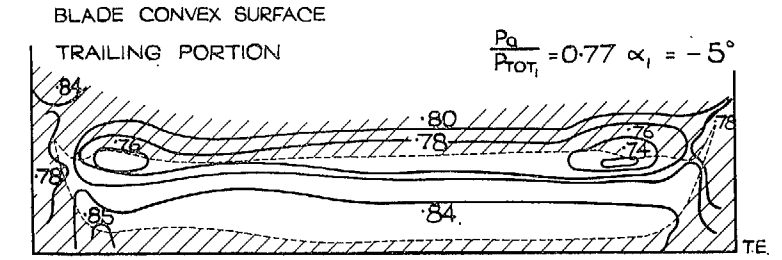

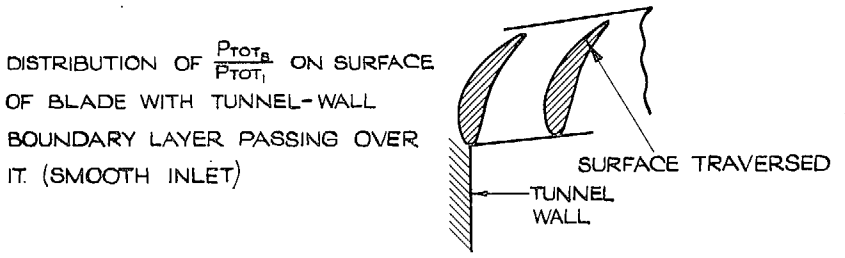

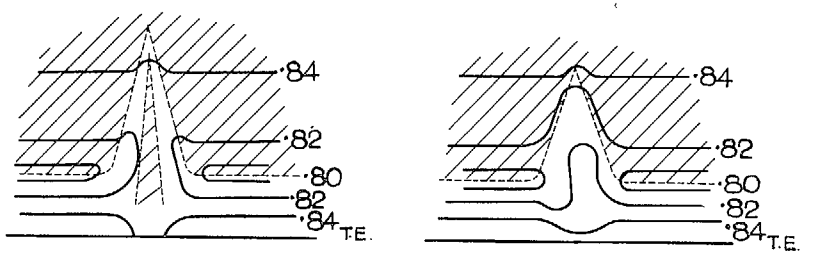

EFFECT OF TWO TYPES OF TURBULENCE WEDGE ON CONTOURS OF $\frac{P_{TOT_2}}{P_{TOT_1}}$

FIG. 6. III Blade surface total-pressure measurements.

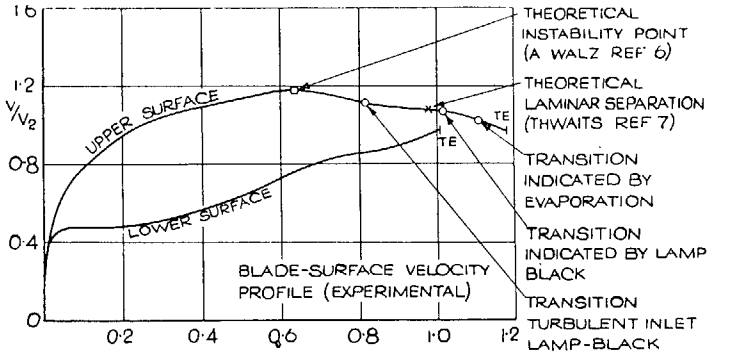

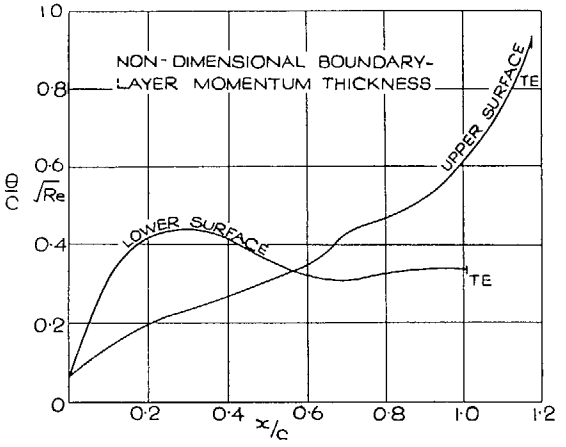

FIG. 7. Blade velocity and boundary-layer momentum thickness distribution.

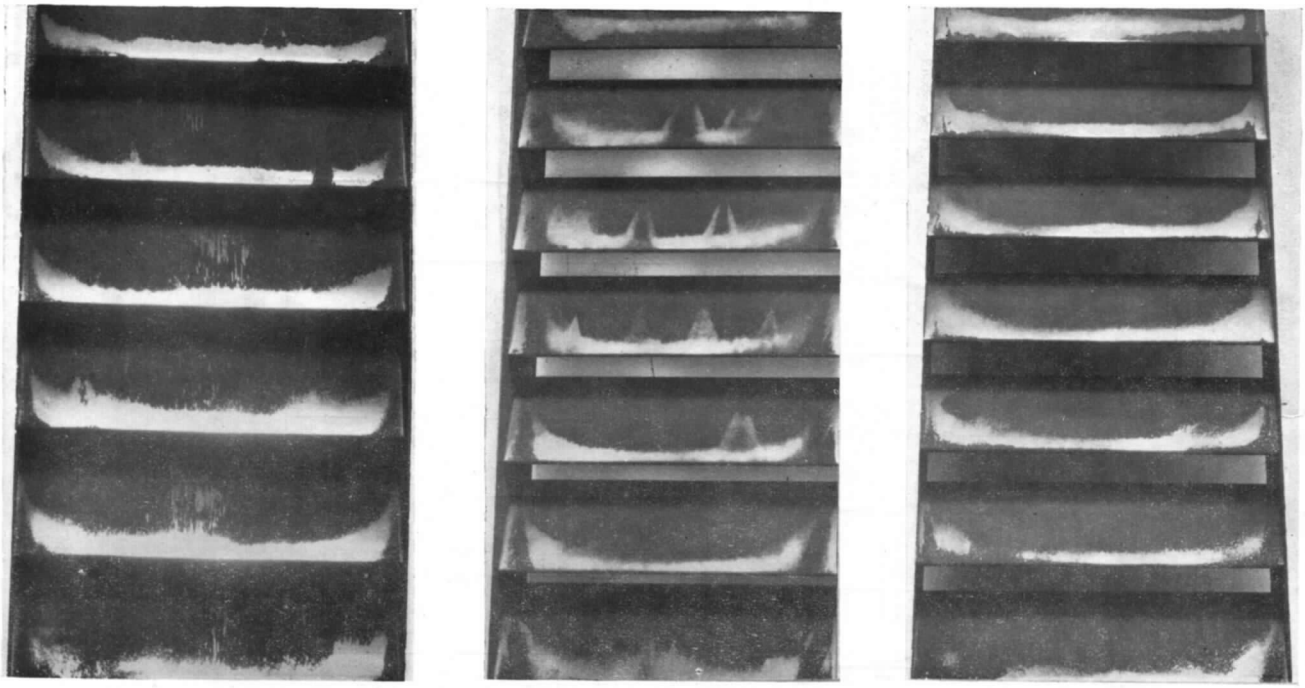

$\alpha_1 = -34{\cdot}5$
Convex surface

$\alpha_1 = -19{\cdot}5$
Convex surface

$\alpha_1 = -4{\cdot}5$
Convex surface

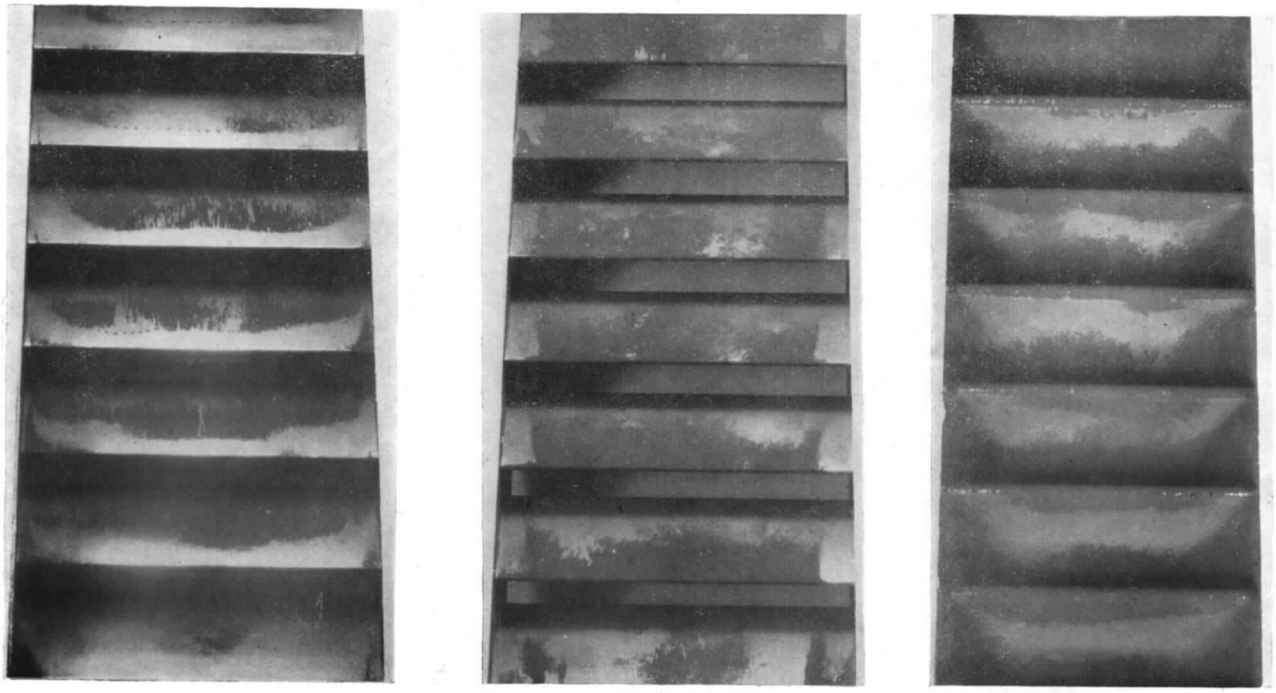

$\alpha_1 = +19{\cdot}5$
Convex surface

$\alpha_1 = +34{\cdot}5$
Convex surface

$\alpha_1 = -34{\cdot}5$
Concave surface

FIG. 8. The effect of incidence on transition (smooth inlet).

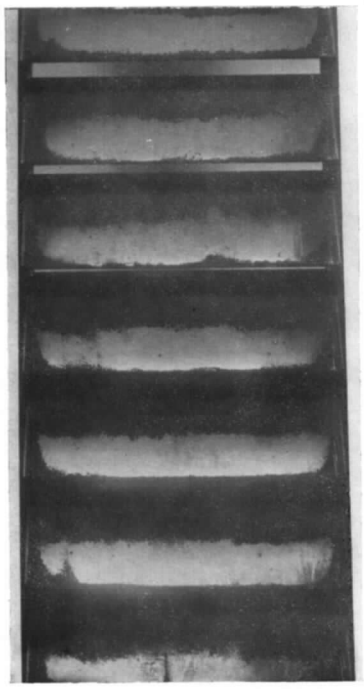

$\alpha_1 = -4{\cdot}5$
Turbulent inlet

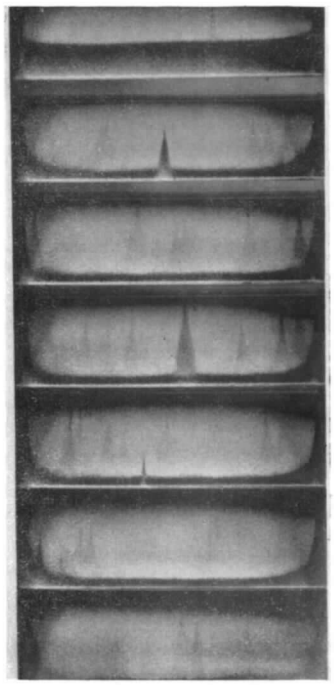

$\alpha_1 = -4{\cdot}5$
Evaporation method

FIG. 9. Transition line.

(6035) Wt. 15/680 K.7 1/56 H.P.Co. 34-261

PRINTED IN GREAT BRITAIN

Publications of the Aeronautical Research Council

ANNUAL TECHNICAL REPORTS OF THE AERONAUTICAL RESEARCH COUNCIL (BOUND VOLUMES)—

1938 Vol. I. Aerodynamics General, Performance, Airscrews. 50*s.* (51*s.* 2*d.*)
Vol. II. Stability and Control, Flutter, Structures, Seaplanes, Wind Tunnels, Materials. 30*s.* (31*s.* 2*d.*)

1939 Vol. I. Aerodynamics General, Performance, Airscrews, Engines. 50*s.* (51*s.* 2*d.*)
Vol. II. Stability and Control, Flutter and Vibration, Instruments, Structures, Seaplanes, etc. 63*s.* (64*s.* 2*d.*)

1940 Aero and Hydrodynamics, Aerofoils, Airscrews, Engines, Flutter, Icing, Stability and Control, Structures, and a miscellaneous section. 50*s.* (51*s.* 2*d.*)

1941 Aero and Hydrodynamics, Aerofoils, Airscrews, Engines, Flutter, Stability and Control, Structures. 63*s.* (64*s.* 2*d.*)

1942 Vol. I. Aero and Hydrodynamics, Aerofoils, Airscrews, Engines. 75*s.* (76*s.* 3*d.*)
Vol. II. Noise, Parachutes, Stability and Control, Structures, Vibration, Wind Tunnels. 47*s.* 6*d.* (48*s.* 8*d.*)

1943 Vol. I. Aerodynamics, Aerofoils, Airscrews. 80*s.* (81*s.* 4*d.*)
Vol. II. Engines, Flutter, Materials, Parachutes, Performance, Stability and Control, Structures. 90*s.* (91*s.* 6*d.*)

1944 Vol. I. Aero and Hydrodynamics, Aerofoils, Aircraft, Airscrews, Controls. 84*s.* (85*s.* 8*d.*)
Vol. II. Flutter and Vibration, Materials, Miscellaneous, Navigation, Parachutes, Performance, Plates and Panels, Stability, Structures, Test Equipment, Wind Tunnels. 84*s.* (85*s.* 8*d.*)

ANNUAL REPORTS OF THE AERONAUTICAL RESEARCH COUNCIL—

1933–34	1*s.* 6*d.* (1*s.* 8*d.*)	1937	2*s.* (2*s.* 2*d.*)
1934–35	1*s.* 6*d.* (1*s.* 8*d.*)	1938	1*s.* 6*d.* (1*s.* 8*d.*)
April 1, 1935 to Dec. 31, 1936	4*s.* (4*s.* 4*d.*)	1939–48	3*s.* (3*s.* 2*d.*)

INDEX TO ALL REPORTS AND MEMORANDA PUBLISHED IN THE ANNUAL TECHNICAL REPORTS, AND SEPARATELY—

April, 1950 . . . . . R. & M. No. 2600 2*s.* 6*d.* (2*s.* 7½*d.*)

AUTHOR INDEX TO ALL REPORTS AND MEMORANDA OF THE AERONAUTICAL RESEARCH COUNCIL—

1909–January, 1954 . . . R. & M. No. 2570 15*s.* (15*s.* 4*d.*)

INDEXES TO THE TECHNICAL REPORTS OF THE AERONAUTICAL RESEARCH COUNCIL—

December 1, 1936 — June 30, 1939	R. & M. No. 1850	1*s.* 3*d.* (1*s.* 4½*d.*)
July 1, 1939 — June 30, 1945	R. & M. No. 1950	1*s.* (1*s.* 1½*d.*)
July 1, 1945 — June 30, 1946	R. & M. No. 2050	1*s.* (1*s.* 1½*d.*)
July 1, 1946 — December 31, 1946	R. & M. No. 2150	1*s.* 3*d.* (1*s.* 4½*d.*)
January 1, 1947 — June 30, 1947	R. & M. No. 2250	1*s.* 3*d.* (1*s.* 4½*d.*)

PUBLISHED REPORTS AND MEMORANDA OF THE AERONAUTICAL RESEARCH COUNCIL—

Between Nos. 2251–2349	R. & M. No. 2350	1*s.* 9*d.* (1*s.* 10½*d.*)
Between Nos. 2351–2449	R. & M. No. 2450	2*s.* (2*s.* 1½*d.*)
Between Nos. 2451–2549	R. & M. No. 2550	2*s.* 6*d.* (2*s.* 7½*d.*)
Between Nos. 2551–2649	R. & M. No. 2650	2*s.* 6*d.* (2*s.* 7½*d.*)

Prices in brackets include postage

HER MAJESTY'S STATIONERY OFFICE

York House, Kingsway, London, W.C.2; 423 Oxford Street, London, W.1 (Post Orders: P.O. Box 569, London, S.E.1); 13a Castle Street, Edinburgh 2; 39 King Street, Manchester 2; 2 Edmund Street, Birmingham 3; 109 St. Mary Street, Cardiff; Tower Lane, Bristol 1; 80 Chichester Street, Belfast *or through any bookseller*

S.O. Code No. 23–2883